

Achromatic optical diode in fiber optics

Michał Berent

Faculty of Physics, Adam Mickiewicz University, Umultowska 85, 61-614 Poznań, Poland*

Andon A. Rangelov and Nikolay V. Vitanov

Department of Physics, Sofia University, James Bourchier 5 Blvd., 1164 Sofia, Bulgaria

We propose a broadband optical diode, which is composed of one achromatic reciprocal quarter-wave plate and one non-reciprocal quarter-wave plate, both placed between two crossed polarizers. The presented design of achromatic wave plates relies on an adiabatic evolution of the Stokes vector, thus, the scheme is robust and efficient. The possible simple implementation using fiber optics is suggested.

PACS numbers: 42.15.Eq, 42.79.-e, 42.81.-i, 78.20.Fm, 78.20.Lm

I. INTRODUCTION

An optical isolator (optical diode) is an optical component that allow the light to pass in one direction but block it in the opposite direction. These devices are commonly used in laser technology to prevent the unwanted back-reflections which might be harmful to optical instrumentation. The standard optical isolator, as first proposed by Rayleigh [1], is composed of two polarizers with their transmission axes rotated by 45° with respect to each other and a Faraday rotator. The Faraday rotator is made of a magnetoactive medium which is placed inside a strong magnet. The magnetic field induces a circular anisotropy in the material (Faraday effect), which makes the left and right circular polarizations experience a different refraction index. As a result, the plane of linear polarization travelling through the device is rotated by an angle equal to

$$\theta(\lambda) = \nu(\lambda)BL, \quad (1)$$

where B is the induction of the applied magnetic field, L is a length of the magnetoactive medium and $\nu(\lambda)$ is the Verdet material constant. Because the Verdet constant depends strongly on the wavelength, so does the rotation angle of the rotator.

The standard optical diode shown in Fig.1 works as follows. The light travelling in the forward direction is first linearly polarized in the horizontal direction by the input polarizer. Afterwards, the Faraday element rotates the polarization by 45° and finally, the light is transmitted through the output polarizer. The light travelling backwards is first linearly polarized at 45°, the Faraday rotator then rotates the polarization by another 45°, meaning the light is now polarized in the vertical direction. Because the input polarizer transmits only horizontal polarization, the light is extinguished. The main drawback of standard isolators is that they work efficiently only

for a very narrow range of wavelengths, because of the dispersion of the Faraday rotation angle $\theta(\lambda)$.

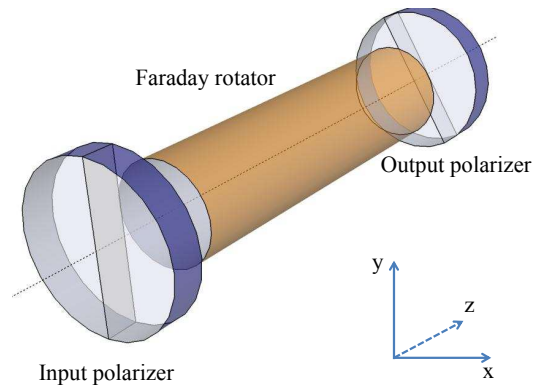


FIG. 1: (Color online) The scheme of a standard Faraday isolator. The light travelling forwards is first polarized in the vertical direction, then the plane of polarization is rotated by 45° by the Faraday rotator and passes through the output polarizer. The light travelling backwards is first polarized at 45°, then it is rotated by another 45° in the Faraday element. The resulting horizontal polarization is extinguished by the input vertical polarizer.

The usual approach seen in commercial broadband isolators is to add the additional reciprocal rotator (e.g. quartz rotator) next to the Faraday rotator. The former element is used to compensate for the dispersion of the Faraday rotator [2–6]. In the forward direction, the rotation of the two elements add up to a total rotation of 90°, whereas in the opposite direction the rotations subtract and no rotation is experienced by the plane of linear polarization.

Recently we proposed a novel broadband isolator [7], which could be realized with the bulk optics elements. We exploited the analogy in the mathematical description of a quantum two-state system driven by a pulsed laser field and an electromagnetic wave propagating through an anisotropic medium. The technique of composite pulses known from nuclear magnetic resonance

*Electronic address: mkberent@gmail.com

(NMR) [8, 9] and quantum optics [10] was applied by us to find conditions for broadband operation of the isolator.

In this article, we propose an alternative realization of an optical isolator which could be suitably implemented in fiber optics. Our approach is based on the adiabatic evolution of the Stokes vector [11, 12] which allows for a broadband performance of the presented isolator.

As high-power fiber lasers are attracting an increasing attention, the development of integrated optical elements for the manipulation of the state of light becomes a crucial point. An all-fiber architecture has the advantage of allowing for an efficient transmission of light without reflections losses on the way (except from an input to a fiber); such losses are a serious problem in bulk optics. As the broadband high-power sources like superluminescent diodes (SLD) or Ti:Sapphire oscillators are broadly used in optical coherence tomography (OCT) [13, 14], characterization of optical components [15] and optical measurements [16], the issue of the efficient broadband isolation in fibers is of increasing importance.

The composition of the manuscript is the following. In the section II we present the mathematical description underpinning our approach. Section III discusses the design of our broadband optical isolator. Then we consider the practical realization of the proposed design in section IV. Section V presents the performance of the diode and in the last section VI we summarize the conclusions.

II. STOKES FORMALISM

Consider the propagation of a plane electromagnetic wave through an anisotropic dielectric medium along the z -axis. We assume that there are no polarization dependent losses. Then the equation of motion is given by the torque equation [17–21]

$$\frac{d}{dz} \mathbf{S}(z) = \boldsymbol{\Omega}(z) \times \mathbf{S}(z) \quad (2)$$

where $\mathbf{S}(z) = [S_1(z), S_2(z), S_3(z)]$ is the Stokes polarization vector representing any state of polarization on the Poincaré sphere, and $\boldsymbol{\Omega}(z) = [\Omega_1(z), \Omega_2(z), \Omega_3(z)]$ is a birefringence vector of the medium. One can write down Eq.(2) in matrix form as

$$\frac{d}{dz} \mathbf{S}(z) = \mathbf{H}(z) \cdot \mathbf{S}(z), \quad (3)$$

where the matrix $\mathbf{H}(z)$ is given as

$$\mathbf{H}(z) = \begin{bmatrix} 0 & -\Omega_3(z) & \Omega_2(z) \\ \Omega_3(z) & 0 & -\Omega_1(z) \\ -\Omega_2(z) & \Omega_1(z) & 0 \end{bmatrix}. \quad (4)$$

We shall make use of the adiabatic evolution of the Stokes vector. For this purpose, we need the eigenvalues of $\mathbf{H}(z)$, which read

$$\varepsilon_-(z) = -i|\Omega(z)|, \quad \varepsilon_0(z) = 0, \quad \varepsilon_+(z) = i|\Omega(z)|, \quad (5)$$

with $|\Omega(z)| = \sqrt{\Omega_1^2(z) + \Omega_2^2(z) + \Omega_3^2(z)}$. The eigenvector that corresponds to the zero eigenvalue is extremely simple:

$$\sigma(z) = \frac{\Omega_1(z)S_1(z) + \Omega_2(z)S_2(z) + \Omega_3(z)S_3(z)}{|\Omega(z)|}. \quad (6)$$

We will call this eigenvector “polarization dark state” in analogy to the stimulated Raman adiabatic passage (STIRAP) process in quantum optics [22–24]. Assuming that the evolution is adiabatic and that the Stokes polarization vector $\mathbf{S}(z)$ is initially aligned with the polarization “dark state” $\sigma(z)$, then the Stokes vector will follow this adiabatic state throughout the medium. The evolution of the polarization “dark state” depends on the initial polarization and the spatial ordering of the components of birefringence vector. It will be discussed in detail in the next section.

In analogy to the quantum-optical STIRAP [23, 24] the condition for adiabatic evolution requires the integral of the length of birefringence vector over the propagation distance L to be large, i.e.

$$\int_0^L |\Omega(z)| dz \gg 1. \quad (7)$$

III. THE DESIGN OF WAVE-PLATES

The optical isolator we are going to present requires two crossed polarizers and two achromatic optical elements: a reciprocal (standard) quarter wave plate and a non-reciprocal quarter wave plate. Below we will describe the design in the framework of formalism presented above.

A. Reciprocal quarter wave-plate

Let us first analyze the operation of the achromatic reciprocal quarter wave-plate. This problem was recently studied in [25, 26]. The reciprocity of the wave plate comes from the reciprocity of the birefringence vector. This means that when the light travels through the wave plate in the reverse direction, the sign of the birefringence vector is also reversed.

Bearing this in mind, we analyze the evolution of the polarization dark state Eq.(6). Let us assume that initially the light is linearly polarized in the horizontal direction, $\mathbf{S}(z_i) = [1, 0, 0]$. When $\Omega_1(z)$ precedes $\Omega_2(z)$ and $\Omega_3(z)$, and the Stokes vector smoothly follows the birefringence vector, the polarization ends up in the right circular polarization state $\mathbf{S}(z_f) = [0, 0, 1]$, provided that only $\Omega_3(z) > 0$ is present at the end (e.g. through a large spin rate of the fiber [25, 26]). The process is fully reversible, meaning that if we change the ordering

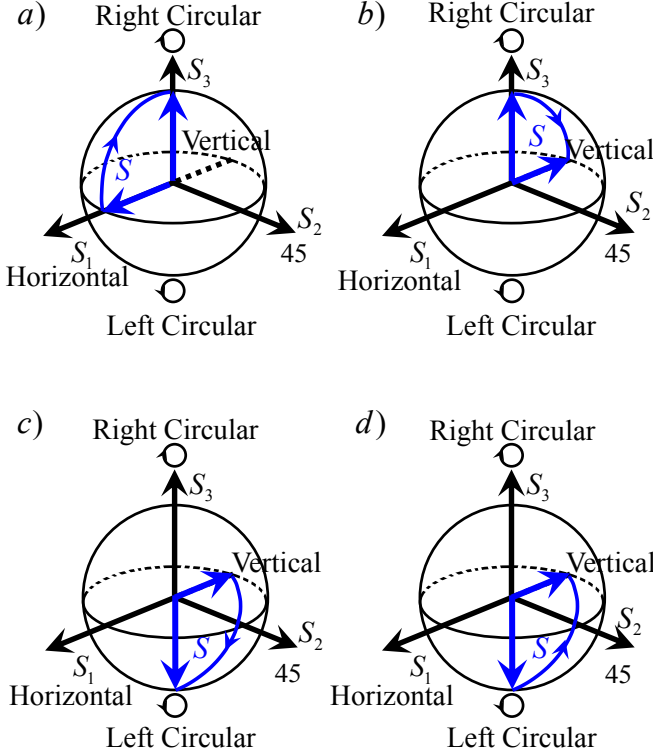


FIG. 2: (Color online) Non-reciprocal polarization transformation propagation. Top frames demonstrate the forward polarization evolution along the direction of the fixed magnetic field: a) Starting from horizontally polarized light and passing through the achromatic reciprocal wave plate leads to right-circular polarization. b) Polarization is evolved from right-circular polarization to vertical, due to the achromatic non-reciprocal wave plate. Bottom frames demonstrate the backward polarization evolution against the direction of the fixed magnetic field: c) Starting from vertical polarization and passing through the achromatic non-reciprocal wave plate the light evolves into left-circular polarization. d) Light pass through the achromatic reciprocal wave plate and, thus, it is returned to vertical polarization.

of the birefringence vector components ($\Omega_3(z)$ now precedes $\Omega_1(z)$ and $\Omega_2(z)$), and the Stokes vector is initially aligned along S_3 -axis, it adiabatically evolves into state $\mathbf{S}(z_f) = [1, 0, 0]$ (horizontal linear polarization). The latter holds if only $\Omega_1(z_f) > 0$ is present at the end. Thus, this arrangement operates as the standard quarter wave plate.

B. Non-reciprocal quarter wave-plate

The second case of the non-reciprocal quarter wave plate requires the use of a non-reciprocal birefringent element, which would be sensitive to the direction of prop-

agation of light. It is long known that the magnetic field applied to a magnetoactive medium induces a circular birefringence which makes the left and right circularly polarized light experience different refractive indices resulting in rotation of the plane of linear polarization.

In the forward direction the operation of the element with one of the birefringence components being non-reciprocal is the same as for a reciprocal one: the light initially polarized horizontally $\mathbf{S}(z_i) = [1, 0, 0]$ is transformed into the right circular polarization state $\mathbf{S}(z_f) = [0, 0, 1]$. However, the propagation in the reverse direction is different. If we start with the right circular polarization $\mathbf{S}(z_i) = [0, 0, 1]$ it evolves into the linear vertical polarization $\mathbf{S}(z_f) = [-1, 0, 0]$ (see Fig. 2).

IV. PRACTICAL IMPLEMENTATION

The design of the broadband optical isolator described in section III could be conveniently implemented with single-mode optical fiber. The use of fiber-optic isolator is exceedingly attractive for integrated fiber-optic systems as well as high power applications.

The single-mode fiber has to exhibit both linear and circular birefringence. The first one might be induced by stress applied to a fiber or by external electric field [12, 27]. To induce the circular birefringence one might apply a torsion of the fiber (for the reciprocal effect) or the external magnetic field (through the Faraday non-reciprocal effect). The possible implementation is depicted in Fig. 3.

The achromatic wave-plate described in section III A would be implemented in the single-mode fiber with the combined stress-induced linear birefringence and torsion of the fiber which would generate a circular birefringence. The choice of torsion-induced circular birefringence is dictated by the requirement that this part of our setup must be reversible.

The first author that experimentally demonstrated the achromatic and adiabatic quarter-wave plate was Huang [25, 26] used a spun fiber with the spinning rate increased with the distance. Those reciprocal designs allowed for the transformation of polarization from linear to circular and back. The reciprocal achromatic quarter-wave plate could be alternatively realized with commercially available achromatic quarter-wave plate.

The non-reciprocal achromatic quarter wave plate can be made similarly to the reciprocal one. The only difference is that one has to use circular birefringence which would be non-reciprocal with respect to the direction of propagation of light. As pointed out earlier, the magnetic field generates such birefringence through the Faraday effect. Similarly to the Faraday rotator in the standard isolator, this element is crucial for the design of the practical optical diode. The problem with the Faraday effect in standard silica fibers is that the Verdet constant of the medium is very low [28] and, thus, one needs a very long piece of fiber or very strong magnetic field to achieve a

significant rotation. Many different approaches have been devised to overcome this difficulty. It seems that the most successful is the doping of fiber with rare-earth ions like terbium (Tb^{3+}). The value of Verdet constant achievable with these fibers [29–31] is nearly as high as that of the bulk optics rotators made of Terbium Gallium Garnet (TGG) [32].

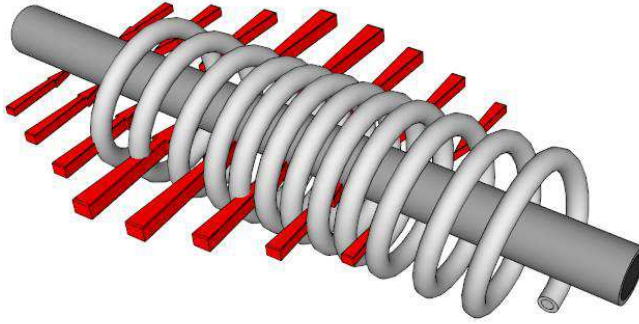


FIG. 3: (Color online) Fiber optics setup of the achromatic quarter wave plate with overlapping linear stress-induced birefringence and circular birefringence generated through the Faraday effect (magnetic field along the fiber). The magnitude of the horizontal stress is represented by red arrows varying in length. Analogously, the number of turns in the coil indicate pulse-shaped spatial variations of the longitudinal magnetic field.

V. RESULTS

We performed numerical simulations of the performance of the design we described in this manuscript. In our calculation we assumed the stress-induced birefringence equal to $\beta = \Delta n = 10^{-5}$ which is easily achievable with the existing technology [27]. The linear birefringence component of the birefringence vector is then given by the equation

$$\Omega_1(z) = \frac{2\pi\beta}{\lambda} \sin^2 \left(\frac{\pi z}{L} \right), \quad (8)$$

where L is the length of the stress element.

As mentioned before, the Verdet constant of the standard silica fiber is very low. Thus, we decided to consider the silica fiber doped with paramagnetic terbium ions. The dispersion of such fiber is similar to a bulk optics TGG crystal [33, 34]

$$\nu(\lambda) = \frac{A}{\lambda^2 - \lambda_0^2}, \quad (9)$$

with slightly different fit parameters $A = -19.7 \cdot 10^6 (\text{nm}^2 \text{ rad})/(\text{T} \cdot \text{m})$ and $\lambda_0 = 385 \text{ nm}$ [29]. The circular component of the birefringence vector now reads

$$\Omega_3(z) = \nu(\lambda)B_0 \sin^2 \left(\frac{\pi(z - z_0)}{L} \right), \quad (10)$$

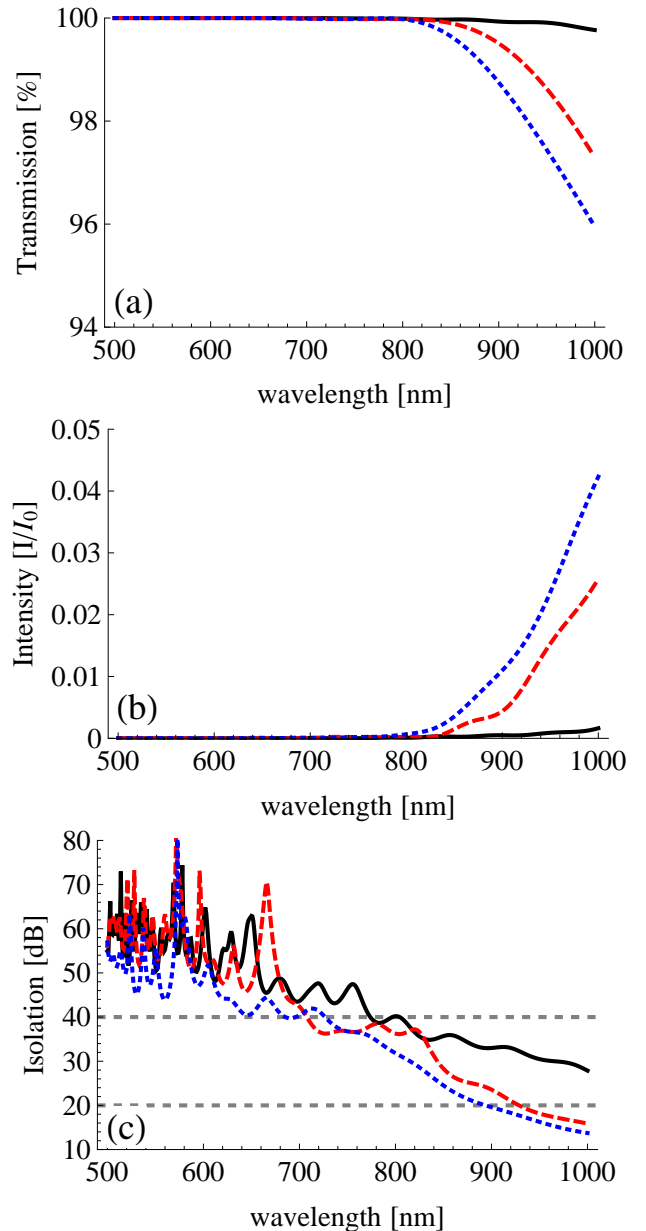


FIG. 4: (Color online) Simulation of the performance of the broadband fiber optical isolator for three different lengths $L_1 = 1.5 \text{ m}$ (black solid line), $L_2 = 1 \text{ m}$ (red dashed line) and $L_3 = 0.7 \text{ m}$ (blue dotted line). We plotted (a) the transmission of the isolator (intensity transmitted in the forward direction), (b) the relative intensity of light travelling in the backward direction, and (c) the isolation of the optical diode, versus wavelength.

with B_0 being the amplitude of the magnetic field induction and z_0 the shift with respect to the linear birefringence. We assumed the magnitude of the magnetic field to be $B_0 = 1 \text{ T}$ and the shift $z_0 = 0.5 \text{ m}$. Simulations were carried out for three different lengths: $L_1 = 1.5 \text{ m}$, $L_2 = 1 \text{ m}$ and $L_3 = 0.7 \text{ m}$.

We quantify the performance of the designed isolator with its transmission and isolation. Transmission indi-

cates the intensity of light passing through the isolator as compared to the intensity at the input. In the forward direction we have

$$T = \frac{I_{forw}}{I_0} = \frac{1}{2} (1 + \mathbf{S}_{forw}^T(z_f) \mathbf{S}_{out}), \quad (11)$$

in the backward direction

$$B = \frac{I_{back}}{I_0} = \frac{1}{2} (1 + \mathbf{S}_{back}^T(z_f) \mathbf{S}_{in}), \quad (12)$$

where $\mathbf{S}_{forw}(z_f)$ represent the Stokes vector of light travelling forwards, $\mathbf{S}_{back}(z_f)$ — for light travelling backwards, $\mathbf{S}_{in} = [1, 0, 0]$ and $\mathbf{S}_{out} = [-1, 0, 0]$ refer to the input horizontal and output vertical polarizers, respectively. Furthermore, I_0 is the intensity of light entering the isolator, whereas I_{forw} and I_{back} are the intensities measured after the diode in the forward and backward directions.

The isolation was calculated using the standard formula [7, 35]

$$D = -10 \log \left(\frac{I_{back}}{I_{forw}} \right). \quad (13)$$

Figure 4 depicts the results of our calculations for the three fiber lengths. In Fig. 4 a and 4 b we present the intensity of light in the forward and backward direction, respectively. One can notice the very broad range of wavelengths where the transmission is maximum and the intensity of back-reflected light minimum (close to zero). Even for the shortest setup considered this plateau is around 300 nm wide.

We also calculated the isolation, which is presented in Fig. 4 c. As the length of the setup decreases the

adiabatic condition is weakened and, thus, the isolation becomes worse.

The isolation of the best commercial broadband fiber diodes [36] is no greater than 32 dB and the range of isolation is around 150 nm. As seen in Fig. 4 c, the isolation of our diode remains greater than 40 dB for a range as wide as 300 nm. Because of the robustness of adiabatic techniques, the isolation would be also insensitive to variations in the temperature and the length of the fiber.

VI. CONCLUSIONS

In this manuscript we proposed a novel design of the fiber optical isolator, which operates over a broad range of wavelengths. The adiabatic evolution has been successfully applied to obtain a robust broadband performance of the optical diode under study. The isolator can be further enhanced by inducing birefringence of higher magnitude. This is possible with stress-induced birefringence, as in our simulations we used a moderate value of the former. To obtain higher circular birefringence with the Faraday effect one can apply stronger magnetic field or use a different magnetooactive medium to assure higher value of the Verdet constant. Increasing the value of birefringence would also result in the decrease of the length of the device.

Acknowledgements

This work is supported by the Bulgarian NSF Grant DMU-03/103.

[1] L. Rayleigh, “On the constant of magnetic rotation of light in bisulphide of carbon”, *Phil. Trans. R. Soc. Lond.* **176**, 343–366 (1885).

[2] H. Iwamura, S. Hayashi, H. Iwasaki, “A compact optical isolator using a $\text{Y}_3\text{Fe}_5\text{O}_{12}$ crystal for near infra-red radiation”, *Opt. Quant. Electr.* **10**, 393–398 (1978).

[3] T. F. Johnston, W. Proffitt, “Design and Performance of a Broad-Band Optical Diode to Enforce One-Direction Traveling-Wave Operation of a Ring Laser”, *IEEE J. Quant. Electr.* **16**, 483–488 (1980).

[4] P. A. Schulz, “Wavelength independent Faraday isolator”, *Appl. Opt.* **28**, 4458–4464 (1989).

[5] P. A. Schulz, “Broadband Faraday Isolator”, U.S. Patent 5,052,786 (1 October 1991).

[6] V. A. Parfenov and V. A. Parfenov, “Broadband Faraday isolator for gravitational wave detectors”, *Class. Quant. Grav.* **19**, 1865–1870 (2002).

[7] M. Berent, A. A. Rangelov and N. V. Vitanov, “Broadband Faraday Isolator”, *Journal of the Optical Society of America A* **30**, 149–153 (2013).

[8] M. H. Levitt and R. Freeman, “NMR Population Inversion Using a Composite Pulse”, *J. Magn. Reson.* **33**, 473–476 (1979).

[9] M. H. Levitt, “Composite pulses”, *Prog. Nucl. Magn. Reson. Spectroscopy* **18**, 61–122 (1986).

[10] B. Torosov and N. V. Vitanov, “Smooth composite pulses for high-fidelity quantum information processing”, *Phys. Rev. A* **83**, 053420 (2011).

[11] A. A. Rangelov, U. Gaubatz, and N. V. Vitanov, “Broadband adiabatic conversion of light polarization”, *Opt. Commun.* **283**, 3891–3894 (2010).

[12] M. Y. Darsht, B. Y. Zeldovich, and N. D. Kundikova, “Achromatic analog of a quarter-wave plate”, *Rus. Phys. Journal* **40**, 71–74 (1997).

[13] E. A. Swanson, J. A. Izatt, M. R. Hee, D. Huang, C. P. Lin, J. S. Schuman, C. A. Puliafito, and J. G. Fujimoto, “In vivo retinal imaging by optical coherence tomography”, *Opt. Lett.* **18**, 1864–1866 (1993).

[14] B. Bouma, G. J. Tearney, S. A. Boppart, M. R. Hee, M. E. Brezinski, and J. G. Fujimoto, “High-resolution optical coherence tomographic imaging using a mode-locked Ti:Al₂O₃ laser source”, *Opt. Lett.* **20**, 1486–1488 (1995).

[15] M. R. Hee, D. Huang, E. A. Swanson, and J. G. Fujimoto, “Polarization-sensitive low-coherence reflectome-

ter for birefringence characterization and ranging”, *J. Opt. Soc. Am. B* **9**, 903–908 (1992).

[16] Th. Udem, R. Holzwarth, and T. W. Hänsch, “Optical frequency metrology”, *Nature* **416**, 233–237 (2002).

[17] W. H. MacMaster, “Matrix Representation of Polarization”, *Rev. Mod. Phys.* **33**, 8–28 (1961).

[18] R. W. Schmieder, “Stokes-Algebra Formalism”, *J. Opt. Soc. Am.* **59**, 297–302 (1969).

[19] H. Kubo and R. Nagata, “Stokes parameters representation of the light propagation equations in inhomogeneous anisotropic, optically active media”, *Opt. Commun.* **34**, 306–308 (1980).

[20] H. Kubo, R. Nagata, H. Kubo, and R. Nagata, “Vector representation of behaviour of polarized light in a weakly inhomogeneous medium with birefringence and dichroism”, *J. Opt. Soc. Am.* **73**, 1719–1724 (1983).

[21] H. Kubo and R. Nagata, “Vector representation of behaviour of polarized light in a weakly inhomogeneous medium with birefringence and dichroism . II . Evolution of polarization states”, *J. Opt. Soc. Am.* **2**, 30–34 (1985).

[22] U. Gaubatz, P. Rudecki, S. Schiemann and K. Bergmann, “Population transfer between molecular vibrational levels by stimulated Raman scattering with partially overlapping laser fields. A new concept and experimental results ”, *J. Chem. Phys.* **92**, 5363–5376 (1990).

[23] K. Bergmann, H. Theuer and B. W. Shore, “Coherent population transfer among quantum states of atoms and molecules ”, *Rev. Mod. Phys.* **70**, 1003–1025 (1998).

[24] N. V. Vitanov, M. Fleischhauer, B. W. Shore and K. Bergmann, “Coherent manipulation of atoms and molecules by sequential pulses ”, *Adv. At. Mol. Opt. Phys.* **46**, 55–190 (2001).

[25] H. C. Huang, “Practical circular-polarization-maintaining optical fiber”, *Appl. Opt.* **36**, 6968–6975 (1997).

[26] H. C. Huang, “Fiber-optic analogs of bulk-optic wave plates”, *Appl. Opt.* **36**, 4241–4258 (1997).

[27] L. A. Fernandes, J. R. Grenier, P. R. Herman, J. S. Aitchison, and P. V. S. Marques, “Stress induced birefringence tuning in femtosecond laser fabricated waveguides in fused silica”, *Opt. Express* **20**, 24103–24114 (2012).

[28] J. L. Cruz, M. V. Andres, and M. a Hernandez, “Faraday effect in standard optical fibers: dispersion of the effective Verdet constant”, *Appl. Opt.* **35**, 922–927 (1996).

[29] J. Ballato and E. Snitzer, “Fabrication of fibers with high rare-earth concentrations for Faraday isolator applications”, *Appl. Opt.* **34**, 6848–6854 (1995).

[30] L. Sun, PhD thesis “All-fiber Faraday Devices Based on Terbium-doped Fiber ”, University of Rochester, Rochester, New York 2010.

[31] L. Sun, S. Jiang, J. D. Zuegel, and J. R. Marciante, “All-fiber optical isolator based on Faraday rotation in highly terbium-doped fiber”, *Opt. Lett.* **35**, 706–708 (2010).

[32] Northrop Grumman Aerospace Systems, http://www.as.northropgrumman.com/products/synoptics_tgg/index.html

[33] T. Hayakawa, M. Nogami, N. Nishi and N. Sawanobori, “ Tb_2O_3 / Dy_2O_3 -Concentrated B_2O_3 - Ga_2O_3 - SiO_2 - P_2O_5 Glasses”, *Chem. Mater.* **14**, 3223–3225 (2002).

[34] E. G. Villora, P. Molina, M. Nakamura, K. Shimamura, T. Hatanaka, A. Funaki, and K. Naoe, “Faraday rotator properties of $Tb_3[Sc_{1.95}Lu_{0.05}](Al_3)O_{12}$, a highly transparent terbium-garnet for visible-infrared optical isolators”, *Appl. Phys. Lett.* **99**, 011111 (2011).

[35] L. Weller, K.S. Kleinbach, M. A. Zantile, S. Knappe, I. G. Hughes, and C. S. Adams, “An optical isolator using an atomic vapor in the hyperfine Pashen-Back regime ”, *Opt. Lett.* **37**, 3405–3407 (2012).

[36] ThorLabs fiber isolators for broadband SLDs, http://thorlabs.com/newgroupage9.cfm?objectgroup_id=4376